Performance improvement of LiMn$_2$O$_4$ as cathode material for lithium ion battery with bismuth modification

C.L. Tan [a,b], H.J. Zhou [a,b], W.S. Li [a,b,*], X.H. Hou [c], D.S. Lü [a,b], M.Q. Xu [a,b], Q.M. Huang [a,b]

[a] *Department of Chemistry, South China Normal University, Guangzhou 510006, China*
[b] *Key Lab of Technology on Electrochemical Energy Storage and Power Generation in Guangdong Universities, Guangzhou 510006, China*
[c] *School of Physics & Telecommunication Engineering, South China Normal University, Guangzhou 510006, China*

ARTICLE INFO

ABSTRACT

Spinel lithium manganese oxides (LiMn$_2$O$_4$) modified with and without bismuth by sol–gel method were investigated by theoretical calculation and experimental techniques, including galvanostatic charge/discharge test (GC), cyclic voltammetry (CV), chronopotentiometry (CP), electrochemical impedance spectroscopy (EIS), inductively coupled plasma (ICP), powder X-ray diffraction (XRD), BET measurement, and infrared spectroscopy (IR). It is found that the performance of LiMn$_2$O$_4$ can be improved by the bismuth modification. The modified and the unmodified samples have almost the same initial discharge capacity, 118 and 120 mAh g^{-1}, respectively. However, the modified sample has better cyclic stability than the unmodified sample. After 100 cycles, the capacity remains 100 and 89 mAh g^{-1} for the modified and the unmodified samples, respectively. Moreover, the results from EIS show that the modified sample has a quicker kinetic process for Li ion intercalation/de-intercalation than the unmodified one; the charge-transfer resistance of the former is less than one-sixth of that of the latter. After immersion in electrolyte (DMC:EC:EMC = 1:1:1, 1 mol L^{-1} LiPF$_6$) for 10 h at room temperature, the modified sample has less change in open circuit potential, crystal volume, and vibration absorption of Mn–O bond, and has less dissolution of manganese into solution than the unmodified sample.

1. Introduction

Lithium manganese oxide, especially spinel LiMn$_2$O$_4$, has been extensively investigated as one of the most promising cathode materials for batteries because manganese compounds have many economical and environmental advantages in preparation and application [1–5]. However, the problem of rapid capacity fading during charging and discharge stands in the way for its wider use [6–10]. Much effort has been devoted to solving this problem and two methods have been proposed to improve the cycling stability so far. One is by doping elements in the lattice of LiMn$_2$O$_4$ to substitute for part of Mn^{3+} ions [11–16]; the other is by coating with various oxides to reduce the contact surface between spinel and electrolyte [17–19].

Dopant, such as Co^{3+}, Cr^{3+} and Al^{3+}, usually has similar radii (55, 62 and 54 pm, respectively) [20–22] with Mn^{3+} (68 pm) [21], so they can enter into the crystal lattice during preparation process and localize in the 16d sites to substitute for part of Mn^{3+} ions. The corresponding effect of Jahn–Teller distortion resulting from Mn^{3+} ions is reduced by the doping. As a result, the integrity of material structure is maintained during the repeated expansion and contraction process, and the cycling stability of the spinel is improved [14]. Unfortunately, the improvement of cycling stability by doping inevitably sacrifices capacity to a great extent.

Coating layer isolates the LiMn$_2$O$_4$ from electrolyte, so that the dissolution of manganese into electrolyte is reduced. However, the capacity of the LiMn$_2$O$_4$ fades due to coating agents. On the other hand, much coating agent has to be used to cover LiMn$_2$O$_4$ in the preparation of oxide-coated materials; for example about 3% mol ratio of TiO$_2$/LiMn$_2$O$_4$ was used to wrap the LiMn$_2$O$_4$ in the synthesis of TiO$_2$-coated material [17] and the same quality of ethyl silicate to get SiO$_2$-coated LiMn$_2$O$_4$ [19].

A new method, bismuth modification, was proposed to improve the spinel stability in this paper. This method is different to the doping as well as the coating, because Bi^{3+} whose radii is 124 pm [23] is too big to enter the spinel lattice and its amount (the molar ratio of Bi/Mn is 0.015) is not enough to cover the whole surface of LiMn$_2$O$_4$ particles. The unmodified and modified LiMn$_2$O$_4$ samples were synthesized and their performance were characterized by using electrochemical impedance spectroscopy (EIS), inductively coupled

* Corresponding author at: Department of Chemistry, South China Normal University, Guangzhou 510006, China. Tel.: +86 20 39310256; fax: +86 20 39310256.
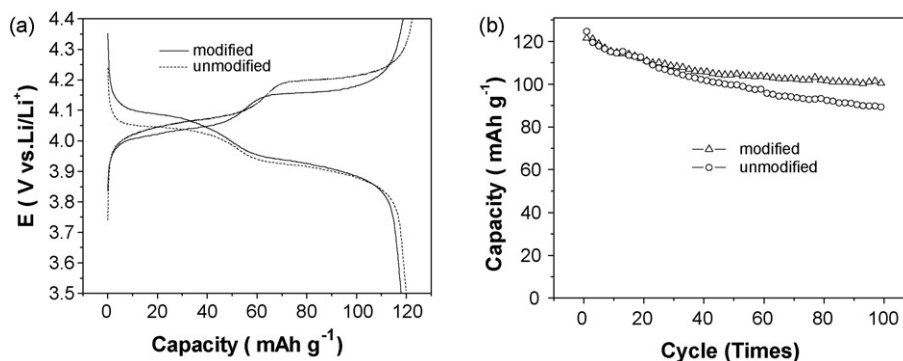*E-mail address:* liwsh@scnu.edu.cn (W.S. Li).

Fig. 1. First charge–discharge curves (a) and cyclic stability (b) of coin cells with modified and unmodified samples, tested on coin cells with a constant current of 40 mA g^{-1}.

plasma (ICP), powder X-ray diffraction (XRD), infrared spectroscopy (IR) and BET.

The lattice parameter and unit cell volume of spinel was calculated by plane wave pseudo-potential method using Cambridge serial total energy package (CASTEP) program.

2. Experimental

Unmodified LiMn$_2$O$_4$ powders were prepared by the sol–gel method using citric acid as a chelating agent. Stoichiometric CH$_3$COOLi·2H$_2$O and Mn(CH$_3$COO)$_2$·4H$_2$O were dissolved in solution containing C$_6$H$_8$O$_7$·2H$_2$O, at 1:1 molar ratio with the total metal ions. All the reagents are analytical grade. The solution was strongly stirred for 4 h at 80 °C at pH 6–7 controlled by adding ammonium hydroxide solution [NH$_3$·H$_2$O (AR, 25%)] and then heating in air to dry. The precursor was annealed at 500 °C for 5 h to remove the organic composition and then sintered at 800 °C for 24 h, followed by grinding in an agate bowl.

The synthesis of modified LiMn$_2$O$_4$ powder (prepared with sol–gel method) is the same as the unmodified LiMn$_2$O$_4$ powder except bismuth ion solution addition. Bismuth nitrate (Bi(NO$_3$)$_3$·5H$_2$O) was dissolved in nitric acid (pH 1) in order to avoid the Bi^{3+} hydrolyzation. The solution was then added slowly to the lithium acetate and manganese acetate (ensuring Bi/Mn molar ratio of 0.015) mixture solutions (Li/Mn = 1:2). The further steps were same as the unmodified LiMn$_2$O$_4$ preparation.

The cycling stability of the samples was tested with coin cell (CR2016). The positive electrodes of the cell were prepared by coating the mixture (80% sample, 10% acetylene black and 10% polyvinylidene fluoride) onto an aluminum foil collector (10 mm in diameter), with NMP (N-methylpyrrolidone) as the solvent. The electrodes were dried at 120 °C for 24 h in vacuum before use. A lithium foil was used as the negative.

The coin cell and the electrochemical cell were assembled in an Ar-filled glove box in 1 M LiPF$_6$ in the 1:1:1 mixture solution of ethylene carbonate (EC), dimethyl carbonate (DMC), and ethyl and methyl carbonate (EMC) as electrolyte.

An abrasive microelectrode [24] was used to get electrochemical information on the spinel samples more quickly and accurately in this paper. With the use of an abrasive electrode, large ratio of sample surface to electrolyte volume can be available and the equilibrium for the interaction between the spinel and the electrode can be reached quickly. Besides, the abrasive electrode contained only spinel, thus the interference from the binder and conductor, which should be used in conventional electrode, can be avoided. The abrasive microelectrode was prepared as follows [25]: a platinum microdisk electrode (with a diameter of 300 μm) was polished on 800- and 2000-grit silicon carbide papers, respectively, cleaned in distilled water ultrasonically for 1 h. Then the electrode was dried and ground on the electrode surface with samples, so that the samples were tightly attached on the surface of platinum microdisk electrodes and the abrasive microelectrodes were obtained. In the application of the abrasive electrode, an electrochemical cell was used with the abrasive electrode as the working electrode and a lithium foil as the counter electrode as well as reference electrode.

The electrochemical experiments were conducted on PGSTAT 30 (Autolab) controlled by GPES and FRA software. For the galvanostatic charge/discharge tests, a constant current of 40 mA g^{-1} was used. For the cyclic voltammetry, the potential range was 3.5–4.5 V with scan rate 10 mV s^{-1}. For the impedance measurement, the electrode was charged to 4.1 V with a very small current of 15 mA and then polarized at 4.1 V for 20 min. The frequency range was 5 mHz to 100 kHz with an amplitude of 5 mV. All electrochemical measurements were carried out at room temperature. The potentials in this paper are all with respect to Li/Li$^+$.
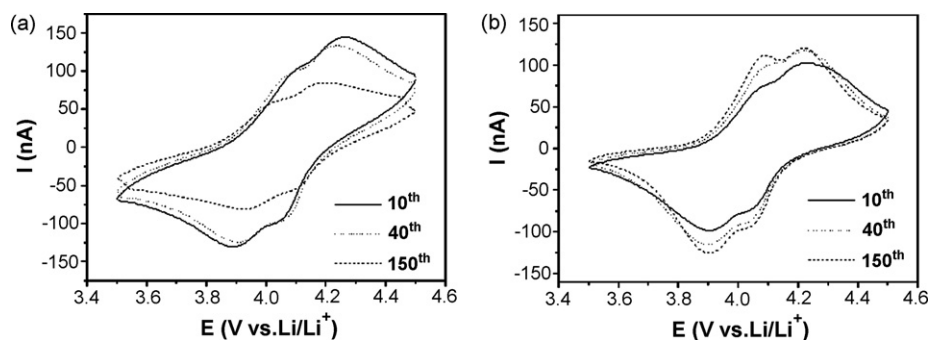

Fig. 2. Cyclic voltammograms of unmodified (a) and modified (b) samples in the potential range of 3.5–4.5 V at 10 mV s^{-1}.
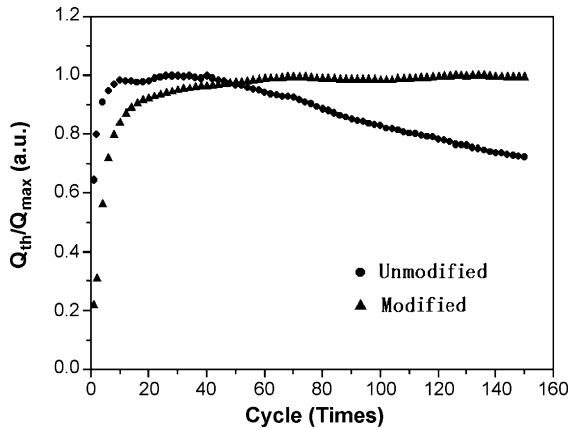
Fig. 3. Relative capacity for two samples calculated from cyclic voltammetric experiments. Q_{th} is the discharge electric quantity of the appointed cycle, while Q_{max} the maximum discharge electric quantity of all cycles.

In ICP, XRD and IR experiments, the samples of 0.5 g were immersed in 13 mL DMC + EC + EMC (1:1:1) + 1 M LiPF$_6$ for 10 h in Ar-filled glove box at room temperature and then the mixture was filtrated. The filtrated liquid was sampled for the analysis of manganese content in the organic solution by using ICP on IRIS Advantage (Thermo Jarrell Ash Corporation, USA). The filtrated solid was collected for structure determination. XRD was carried out on the Rigaku D/Max-2000 instrument, using Cu Kα radiation and the range of diffraction angle (2θ) was from 10° to 70°. FTIR was conducted on Admin Spectrum One-69326 using KBr pellets.

3. Results and discussion

Fig. 1 presents the first charge–discharge curves and the cycling ability of the coin cells with modified and unmodified samples. It can be seen from Fig. 1a that the modification of LiMn$_2$O$_4$ with bismuth does not change its charge and discharge characterization: two potential platforms for the lithium ion intercalation or de-intercalation into or from the spinel, for Li$_x$MnO$_4$ $0 \leq x \leq 0.5$ and $0.5 < x \leq 1$, respectively. It is found that there is a little loss in charge or discharge capacity of the modified sample compared with the unmodified sample, the discharge capacity is 118 and 120 mAh g^{-1}, respectively. However, the cycling stability of the spinel has been improved by the modification, as shown in Fig. 1b. After 100 cycles, the discharge capacity remains 100 mAh g^{-1} for the modified sample but only 89 mAh g^{-1} for the unmodified sample.

Fig. 2 shows the cyclic voltammograms of abrasive electrodes with unmodified and modified samples at 10 mV s^{-1} in potential
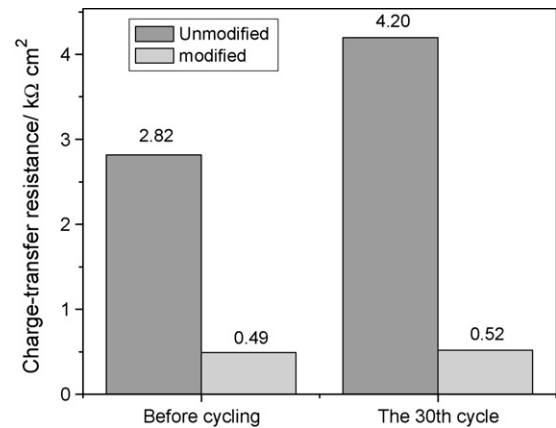

Fig. 5. Charge-transfer resistance of modified and unmodified samples.

range of 3.5–4.5 V. Two typical redox peaks, corresponding to the lithium ion intercalation or de-intercalation into or from the spinel, for Li$_x$MnO$_4$ $0 \leq x \leq 0.5$ and $0.5 < x \leq 1$, respectively, can be observed for both samples.

Fig. 3 shows the change of relative discharge capacity with cycling. The relative discharge capacity (Q_{th}/Q_{max}) is defined as the ratio of discharge electric quantity of appointed cycle (Q_{th}) to the maximum discharge electric quantity (Q_{max}) of all cycles. It can be seen that the two spinel samples delivered small initial capacity and the capacity increases with cycling during the first several cycles. This results from the activation process of spinel in the abrasive electrode under such fast scanning rate. With the cycling increases further, the relative capacity of the unmodified sample decreases quickly. Contrarily, the relative capacity of the modified sample keeps almost constant, indicating that the modified sample has a better cycling stability than the unmodified sample. This is in agreement with the results from the charge–discharge test of coin cells and verifies that the abrasive electrode can be used to compare the cycling stability of spinel samples quickly with cycling voltammetry.

Fig. 4 presents the electrochemical impedance spectra of two samples at 4.1 V before and after 30 cycles. The EIS spectra reflect the steps of the Li$^+$ intercalation process, including the diffusion of Li$^+$ in solution, Li$^+$ migration through the surface film of Li$_x$Mn$_2$O$_4$, charge-transfer for Li$^+$ intercalation, diffusion of Li$^+$ in the solid phase, and occupation of Li in the lattice [26]. The EIS spectra can be well fitted by the equivalent circuit inserted in the figure, where R_s represents the solution resistance, R_f and C_f the film resistance and capacitance, R_{ct} and C_{dl} the charge-transfer resistance and double layer capacitance for Li$^+$ intercalation, respectively, Z_w the diffu-
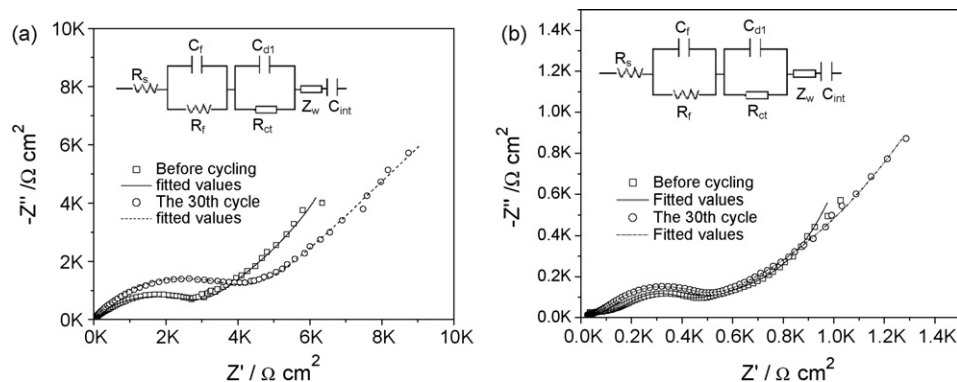

Fig. 4. Impedance spectra of unmodified (a) and modified (b) samples before and after 30 cycles.
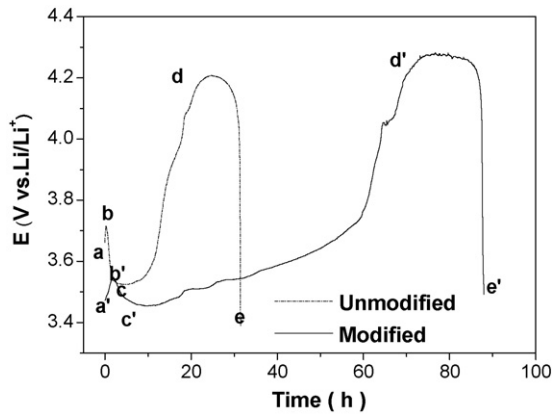
Fig. 6. The variation of open circuit potential (OCP) with time at room temperature.

Fig. 8. Lattice parameters calculated from XRD results.

Table 1
Manganese content in the electrolyte after immersion of samples for 10 h at room temperature

Samples	Mn contents in electrolyte ($mg\,L^{-1}$)	Percentage of manganese dissolution loss (wt.%)
Unmodified	4	0.02
Modified	2.7	0.012

sion impedance of Li^+ in the solid phase, and C_{int} the intercalation capacitance [26].

Fig. 5 shows the charge-transfer resistance obtained by simulating the experimental data with the equivalent circuit. It can be seen from Fig. 5 that the charge-transfer resistance of the unmodified sample is much larger than that of the modified sample before or after 30 cycles. This indicates that the electrode reaction kinetics of the former is more sluggish than that of the later. In addition, the charge-transfer resistance of two samples increases significantly after 30 cycles, but that of the modified sample has less change, from 0.49 to $0.52\,k\Omega\,cm^2$, than that of the unmodified sample, which changes from 2.82 to $4.20\,k\Omega\,cm^2$. This suggests that the electrode process of the modified sample has faster charge-transfer kinetics and is less influenced by cycling than that of the unmodified sample.

Fig. 6 presents the chronopotentiograms of two samples at open circuit potential. In these experiments, potential at open circuit was recorded as the function of time immediately after the cell assembly was completed. The potential changes of two samples have similar trends with time. At the beginning, the potential increases and then decreases quickly to a valley, which is labeled from a or a′ to b or b′, and then to c or c′, as shown in Fig. 6. This change reflects the interaction between the sample and the electrolyte.

The potential changes from c or c′ to d or d′ can be ascribed to a manganese dissolution process [27]:

$$2LiMn_2O_4 + 4H^+ \rightarrow 3\lambda\text{-}MnO_2 + Mn^{2+} + 2Li^+ + 2H_2O \qquad (1)$$

When most fraction of material is converted into λ-MnO_2, the potential reaches its maximum. However, the λ-MnO_2 is very active

to electrolyte and reaction (2) takes place, which corresponds to the potential changed from d or d′ to e or e′ [28].

$$2\lambda\text{-}MnO_2 + xLi^+ + xEl \rightarrow Li_xMn_2O_4 + xEl^+ \quad (0 \leq x \leq 2) \qquad (2)$$
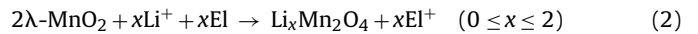
In Eq. (2), El represents EC, EMC, etc. It can be found from Fig. 6 that the time for the potential change of the modified sample from c′ to d′ is about 60 h, far longer than that of the unmodified sample, which is only about 12 h. This indicates that the modified sample has a better chemical stability than that of the unmodified sample. Bismuth is believed to trap the trace HF to form BiF_3 [29]. This reduces the acid in solution and inhibits the manganese dissolution. Due to the improved stability of $LiMn_2O_4$ with bismuth modification, less $Li_xMn_2O_4$ ($0 \leq x \leq 2$) of reaction (2) forms on the surface of the modified sample than the unmodified sample, resulting in quicker charge-transfer process.

To further testify the chemical stability of the samples, 0.5 g of each sample was immersed in 13 mL EC + DMC + EMC (1:1:1) + 1 M $LiPF_6$ for 10 h at room temperature. Then the clear electrolyte that contained dissolved manganese ions was filtrated for ICP analysis. The results of dissolution loss of manganese are shown in Table 1.
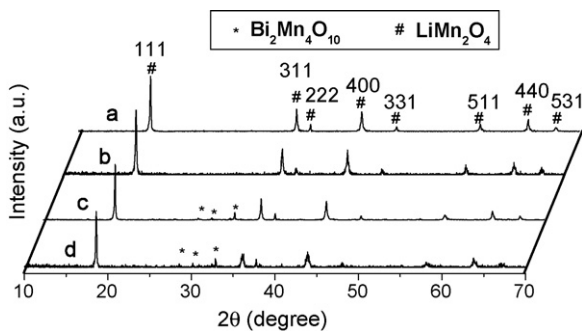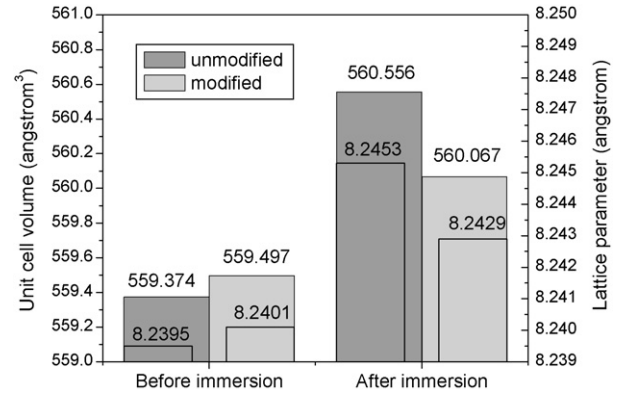

Fig. 7. XRD patterns of unmodified sample before (a) and after (b) immersion, and modified sample before (c) and after (d) immersion.
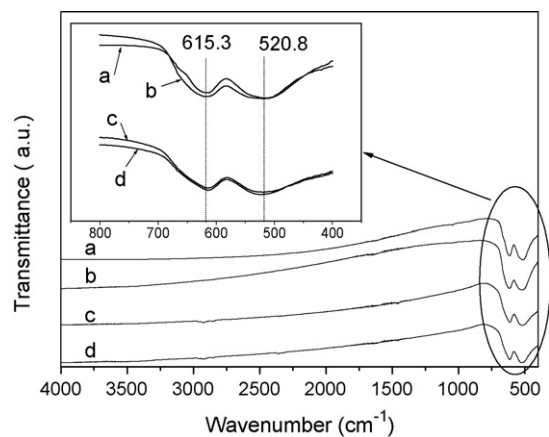

Fig. 9. Infrared spectra of unmodified sample before (a) and after (b) immersion, and modified sample before (c) and after (d) immersion.
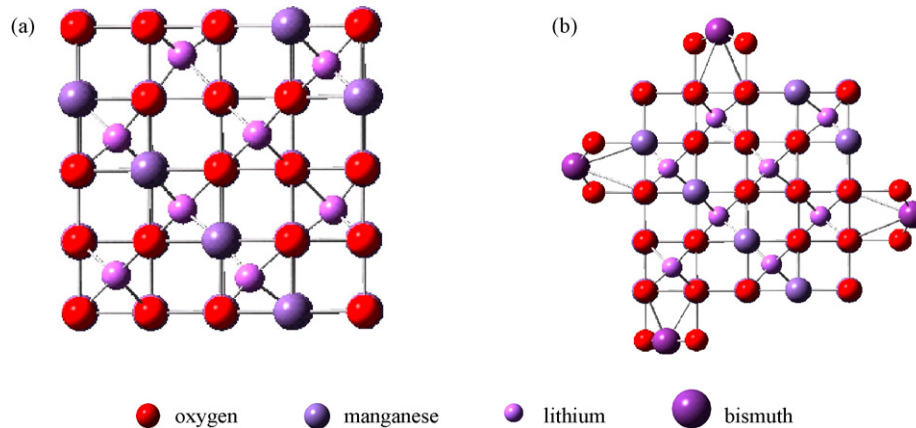
Fig. 10. Schematic representation of structures for unmodified $LiMn_2O_4$ spinel (a) and modified sample (b).

It can be seen that the content of manganese in solution is $4\,mg\,L^{-1}$ for the unmodified sample and $2.7\,mg\,L^{-1}$ for the modified sample, corresponding to the manganese loss of 0.02 wt.% for the unmodified sample and 0.012 wt.% for the modified sample. The content of manganese may be too small to be determined accurately by ICP, but the difference in manganese dissolution between two samples can still be distinguished. It is obvious that the dissolution of $LiMn_2O_4$ can be suppressed with bismuth modification to some extent although it cannot be suppressed completely.

The unmodified and the modified samples before and after immersion experiments were examined by powder X-ray diffraction. The results are shown in Fig. 7. A typical spinel structure can be observed in Fig. 7a, while there appears new weak diffraction of phase $Bi_2Mn_4O_{10}$ [29] besides the strong diffraction of spinel phase in the modified sample (Fig. 7c and d). $Bi_2Mn_4O_{10}$ is inactive to lithium intercalation and de-intercalation and is responsible for the lower initial capacity of the modified sample than that of the unmodified sample. After immersion, all peak intensity was reduced and the peaks were widened. This phenomenon can be ascribed to the changes of lattice integrity due to immersion. The lattice parameters of the samples before and after immersion are shown in Fig. 8. It can be seen from Fig. 8 that after immersion cell volume of the modified sample changes less than that of the unmodified sample. The lattice parameter changes from 8.2395 to 8.2453 Å for the unmodified sample but only from 8.2401 to 8.2429 Å for the modified sample. Thus there is larger cell volume increase in the unmodified sample than in the modified sample due to the immersion. Assuming that bismuth ions enter the lattice of the spinel and occupy the 16d sites to substitute for part of Mn^{3+} ion like Co, Cr or Al ions, the lattice with doping Bi can be calculated by plane wave pseudo-potential method using CASTEP program [30]. The calculated results are shown in Table 2. The unit cell volume of spinel increases by a ratio of 0.28% due to the doping. In fact, the cell volume obtained from XRD increases 0.022% due to the bismuth modification. This confirms that the bismuth in the modified sample does not enter the spinel structure.

Fig. 9 shows the IR spectra of the samples before and after immersion. It can be seen from Fig. 9 that there are two absorption peaks at around 615.3 and $520.8\,cm^{-1}$ for all samples. They belong to the stretching vibration of Mn(IV)–O and Mn(III)–O bond, respectively [31,32]. It can be found, by comparing the absorption peaks of the samples before and after immersion, that the stretching vibration of Mn–O bond in the unmodified sample is broadened due to the immersion, as shown by curves a and b in the inserted plot. However, the immersion hardly changes the stretching vibration of Mn–O bond in the modified sample, as shown by curves c and d. This suggests that the immersion elongates Mn–O bond and thus enlarges the cell volume of the unmodified sample but hardly change those of the modified sample. This is well in agreement with the XRD results.

The cubic spinel $LiMn_2O_4$ possesses a space group of $Fd3m$, in which oxygen atoms occupy the 32e sites, manganese atoms occupy the 16d octahedral sites and lithium atoms occupy the 8a tetrahedral sites [33], as shown in Fig. 10a. Edge-sharing $[MnO_6]$ octahedra form the spinel structural framework, whereas the common faces between each 8a tetrahedron and four neighboring empty octahedra together with four 8f tetrahedra form the three-dimensional network for lithium intercalation and de-intercalation. With the available results, it can be inferred that the stability improvement of $LiMn_2O_4$ with bismuth modification results from the model of an interaction between bismuth and manganese on the surface of the spinel. Bismuth can complex with oxygen atoms of edge-sharing $[MnO_6]$ octahedra [34], as indicated in Fig. 10b, i.e. one Bi ion can grasp one Mn–O–Mn–O square then stabilize the integrity of spinel structure. The quantity of bismuth necessary for the complexion can be calculated from the specific surface area of $LiMn_2O_4$ powder. The specific surface area of pure $LiMn_2O_4$ powder determined by BET measurement is $3.28\,m^2\,g^{-1}$, and bond length of Mn–O bond is $0.24a$ ($a = 8.2395$ Å). About 8.37×10^{19} Bi ions, 1.39×10^{-4} mol, should be required to modify 1 g $LiMn_2O_4$ sample (containing 0.011 mol Mn ions). Thus, the Bi/Mn molar ratio for the surface modification is 0.0126. In this work, the Bi/Mn molar ratio of the modified sample is 0.015, which should provide enough

Table 2
Lattice parameters calculated from XRD (a) and by CASTEP (b)

	Samples	Lattice parameter (Å)	Unit cell volume (Å³)	Volume changes (%)
(a)	Unmodified	8.2395	559.374	–
	Modified	8.2401	559.497	0.022
(b)	Unmodified	8.2383	559.130	–
	Doped	8.2460	560.699	0.28

bismuth to modify the spinel surface. However, the modification is not perfect, though the performance is improved to some extent by the modification. This may be ascribed to the formation of $Bi_2Mn_4O_{10}$. Much effect should be made in the future work for the application of bismuth modification to get better performance of the spinel.

4. Conclusion

With the bismuth modification, the performance of $LiMn_2O_4$ as cathode materials of Li ion battery can be improved. The modified sample has better cycling stability, quicker charge-transfer process and better chemical stability than the unmodified sample. The performance improvement can be attributed to two reasons: one is the trapping of trace HF and the other is the complexion with oxygen atoms of edge-sharing $[MnO_6]$ octahedra. This modification is different from conventional methods to stabilize $LiMn_2O_4$, doping or coating, which need more doping or coating elements and also sacrifice the capacity of $LiMn_2O_4$.

Acknowledgements

References

[1] J.M. Tarascon, M. Armand, Nature 414 (2001) 359–367.
[2] A. Manthiram, J. Kim, Chem. Mater. 10 (1998) 2895–2909.
[3] V.G. Kumar, J.S. Gnanaraj, S. Ben-David, D.M. Pickup, E.R.H. van-Eck, A. Gedanken, D. Aurbach, Chem. Mater. 15 (2003) 4211–4216.
[4] W.S. Li, L.C. Jiang, G.Y. Xie, X. Jiang, J. Power Sources 58 (1996) 235–237.
[5] W.S. Li, L.C. Jiang, Z.T. Huang, J. Power Sources 69 (1997) 81–87.
[6] H. Zhou, P.S. Fedkiw, Electrochim. Acta 48 (2003) 2571–2582.
[7] D.S. Lü, W.S. Li, Acta Chim. Sin. 61 (2003) 225–229.
[8] D. Aurbach, M.D. Levi, K. Gamulski, B. Markovsky, G. Salitra, E. Levi, U. Heider, R. Oesten, J. Power Sources 81–82 (1999) 472–479.
[9] B.J. Hwang, R. Santhanam, D.G. Liu, Y.W. Tsai, J. Power Sources 102 (2001) 326–331.
[10] D.S. Lü, W.S. Li, Chin. J. Inorg. Mater. 19 (2004) 801–808.
[11] I.S. Jeong, J.U. Kim, H.B. Gu, J. Power Sources 102 (2001) 55–59.
[12] J.H. Lee, J.K. Hong, D.H. Jang, Y.-K. Sun, S.M. Oh, J. Power Sources 89 (2000) 7–14.
[13] Z.Y. Chen, Y.R. Li, Z.L. Yu, Chin. Chem. Lett. 14 (2003) 1296–1298.
[14] S.T. Yang, J.H. Jia, L. Ding, M.C. Zhang, Electrochim. Acta 48 (2003) 569–573.
[15] M. Wagemaker, F.G.B. Ooms, E.M. Kelder, J. Schoolman, F.M. Mulder, J. Am. Chem. Soc. 126 (2004) 13526–13533.
[16] R. Alcantara, M. Jaraba, P. Lavela, J.L. Tirado, E. Zhecheva, R. Stoyanova, Chem. Mater. 16 (2004) 1573–1579.
[17] Z.R. Zhang, Z.L. Gong, Y. Yang, J. Phys. Chem. B 108 (2004) 17546–17552.
[18] S.W. Lee, K.S. Kim, H.S. Moon, J.P. Lee, H.J. Kim, B.W. Cho, W.L. Cho, J.W. Park, J. Power Sources 130 (2004) 227–232.
[19] Z.S. Zheng, Z.L. Tang, Z.T. Zhang, W.C. Shen, Y.H. Lin, Solid State Ionics 148 (2002) 317–321.
[20] C.H. Shen, R.S. Liu, R. Gundakaram, J.M. Chen, S.M. Huang, J.S. Chen, C.M. Wang, J. Power Sources 102 (2001) 21–28.
[21] Y.C. Su, Q.F. Zou, Y.W. Wang, P. Yu, J.Y. Liu, Mater. Chem. Phys. 84 (2004) 302–307.
[22] D. Capsoni, M. Bini, G. Chiodelli, V. Massarotti, P. Mustarelli, L. Linati, M.C. Mozzati, C.B. Azzoni, Solid State Commun. 126 (2003) 169–174.
[23] H. Chiba, T. Atou, Y. Syono, J. Solid State Chem. 132 (1997) 139–143.
[24] D.A. Fiedler, J.O. Besenhard, M.H. Fooken, J. Power Sources 69 (1997) 157–160.
[25] H.J. Zhou, D.S. Lü, W.S. Li, M.Q. Xu, Chin. J. Inorg. Mater. 21 (2006) 109–114.
[26] D.S. Lu, W.S. Li, X.X. Zuo, Z.Z. Yuan, Q.M. Huang, J. Phys. Chem. C 111 (2007) 12067–12074.
[27] T. Uchiyama, M. Nishizawa, T. Itoh, I. Uchida, J. Electrochem. Soc. 147 (2000) 2057–2061.
[28] P. Arora, R.E. White, M. Doyle, J. Electrochem. Soc. 145 (1998) 3647–3667.
[29] D. Larcher, P. Courjal, R.H. Urbina, B. Gerand, A. Blyr, A. du Pasquier, J.M. Tarascon, J. Electrochem. Soc. 145 (1998) 3392–3400.
[30] S.J. Clark, M.D. Segall, C.J. Pickard, P.J. Hasnip, M.J. Probert, K. Refson, M.C. Payne, Z. Krystall. (2005) 567–570.
[31] Q. Feng, Y. Miyai, H. Kanoh, K. Ooi, Langmuir 8 (1992) 1861–1867.
[32] C.Q. Feng, K.L. Zhang, J.T. Sun, Spectrosc. Spectral Anal. 23 (2003) 279–281.
[33] B. Ammundsen, J. Rozière, M.S. Islam, J. Phys. Chem. B 101 (1997) 8156–8163.
[34] L.T. Yu, J. Electrochem. Soc. 144 (1997) 802–809.